

M. Phillips, S. Prager, and J. Sprott, *Nucl. Fusion* **9**, 1509 (1979).

<sup>3</sup>H. A. B. Robin and A. A. Newton, *Nucl. Fusion* **20**, 1255 (1980).

<sup>4</sup>B. Lipschultz, S. C. Prager, A. M. M. Todd, and J. Delucia, *Nucl. Fusion* **20**, 683 (1980).

<sup>5</sup>B. B. Kadomtsev, *Fiz. Plazmy* **1**, 710 (1975) [*Sov. J. Plasma Phys.* **1**, 389 (1975)].

<sup>6</sup>J. A. Holmes, B. Carreras, H. R. Hicks, and V. E. Lynch, in *Proceedings of the IEEE International Conference on Plasma Science, Madison, Wisconsin, 1980* (IEEE, New York, 1980), paper 5I7.

## Spatially Resolved Measurements of Fully Ionized Low-Z Impurities in the PDX Tokamak

R. J. Fonck, M. Finkenthal,<sup>(a)</sup> R. J. Goldston, D. L. Herndon, R. A. Hulse, R. Kaita, and D. D. Meyerhofer

*Plasma Physics Laboratory, Princeton University, Princeton, New Jersey 08544*

(Received 14 June 1982)

Fully ionized oxygen and carbon in PDX plasmas are detected via charge-exchange recombination reactions between the impurities and hydrogen atoms from a low-power neutral beam. The C<sup>6+</sup> and O<sup>8+</sup> ions are observed out to radii beyond the limiter, which is in contrast to expectations based on coronal equilibrium but consistent with a simple diffusive transport model. Central values of  $Z_{\text{eff}}$  obtained with these measurements agree with values obtained from plasma resistivity and visible bremsstrahlung measurements.

PACS numbers: 52.70.-m, 34.70.+e, 52.25.Fi

Low- $Z$  elements such as carbon and oxygen are usually the most abundant impurities in tokamak plasmas. At the central electron temperatures in present large tokamaks ( $T_e \sim 1$  to 2 keV), these atoms are fully ionized in the plasma core, and their detection with conventional spectroscopic observations is not possible. The inference of central low- $Z$  impurity behavior from observations of lower-charge-state emissions from the plasma edge region will become increasingly uncertain as  $T_e$  increases to 5 keV and above in the next generation of tokamak devices, such as the tokamak fusion test reactor (TFTR). Thus, direct detection of these fully stripped impurities is necessary.

Since an impurity ion is left in an excited state following charge-exchange recombination between the ion and a hydrogen atom, the process



is useful for detecting the presence of the ion  $\text{Z}^{+q}$  (with charge  $q$ ) by observing the subsequent photon emission from the excited product of the reaction described in Eq. (1). The cross sections for these processes are large ( $\sim 10^{15} \text{ cm}^{-2}$ ), resulting in high emissivities with only a moderate neutral hydrogen density.

Spectral-line excitation from this process was observed during neutral-beam heating in the ORMAK<sup>1</sup> and ISX-B<sup>2</sup> tokamaks. In addition to

perturbing the plasma, high-power neutral-beam heating introduces enough H<sup>0</sup> into the discharge to change the ionization distribution of the impurities themselves.<sup>3,4</sup> It is thus desirable to employ a nonperturbing source of neutrals to induce the reaction [Eq. (1)] as was done in the T-4 and T-10 tokamaks.<sup>5,6</sup> A similar approach has been used on the poloidal divertor experiment (PDX) tokamak and is reported here.

The experimental apparatus for the measurements on PDX includes a highly collimated diagnostic neutral beam (DNB)<sup>7</sup> which provides neutrals in the field of view of an absolutely calibrated grazing incidence spectrometer (Fig. 1). The beam can be scanned across the plasma mid-plane. The neutral hydrogen atoms had a primary energy of 25 keV and a total injected power of 4 to 11 kW. Typical column densities along the line of sight of the spectrometer were  $10^8$  to  $10^9 \text{ cm}^{-2}$ , which results in line intensities on the order of  $10^{12}$  to  $10^{13} \text{ photons/cm}^2 \text{ s sr}$ . The neutral-beam cross section full width at half maximum was 12 cm high and 5 cm wide, while the spatial resolution of the spectrometer in the vertical direction was 2 cm.

The PDX tokamak was run with graphite rail limiters for these experiments; the divertor was not activated. The plasma major radius was 147 cm and the limiter radius was 30 cm. The plasma current was 250 kA, the line-averaged elec-

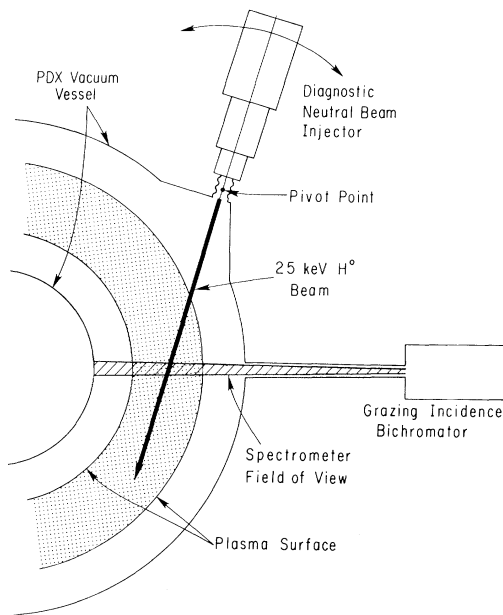


FIG. 1. Schematic of low- $Z$  impurity diagnostic on PDX.

tron density was  $\bar{n}_e = 2.0 \times 10^{13} \text{ cm}^{-3}$  and  $T_e(0) = 830 \text{ eV}$ . Electron density and temperature profiles were obtained from a multipoint Thomson scattering system. Soft x-ray measurements showed no sawtooth activity in these discharges at the time of injection of the DNB.

An example of the charge-exchange-induced signal for the O VIII 102-Å (3-2) spectral line is shown in Fig. 2. The eight 1-ms-long pulses arise from the 500-Hz square-wave modulation of the neutral-beam current, which allows phase-sensitive detection for weak signals. For this spectral line, the modulated intensity was as high as 100% of the intrinsic line intensity, which is due to excitation of  $O^{7+}$  along the spectrometer line of sight. Scanning the spectrometer line of sight vertically across the neutral beam showed that no modulated signal appeared outside the beam position, indicating that the observed modulation is due solely to prompt charge-exchange excitation.

For a fully ionized ion of charge  $Z$ , the charge-exchange process tends to populate the high- $l$  states with the peak cross sections occurring at  $n$  levels given by  $n_{\text{peak}} \sim Z^{0.75}$ . Thus both direct charge exchange and cascades from higher  $n$  levels contribute to the observed line intensities from the  $n=3$  and 4 levels. The cascade-corrected total effective cross section for excitation of various transitions in C VI and O VIII were

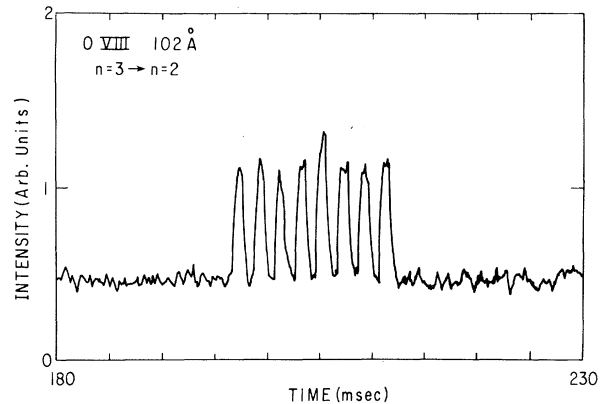


FIG. 2. Excitation of O VIII 102-Å emission by the pulsed diagnostic neutral beam.

calculated with available cross sections. Theoretical cross sections for charge exchange into a given  $(n, l)$  state of C VI have been provided by Green, Shipsey, and Browne<sup>8</sup> over the energy range of interest (0.2 to 25 keV/u). In general, it was found that the ratio of effective cross section for excitation of the 4-3 and 3-2 transitions in C VI to the total charge-exchange cross section (i.e., summed over all  $n, l$ ) was only a weak function of the  $H^0$  energy. The  $(n, l)$  distributions produced by the  $H^0 + O^{8+}$  reaction were not readily available except for the values of Salop<sup>9</sup> at 25 keV. These values were thus used for all energies with the expectation that, as was found for carbon, the ratio of effective cross section for the 3-2 or 4-3 transition to the total charge-exchange cross section is only a weak function of neutral energy. The scaling of the total cross section with energy for  $O^{8+}$  was taken from Ryufuku and Watanabe,<sup>10</sup> normalized to the value of Salop at 25 keV.

The line density of hydrogen neutrals from the diagnostic neutral beam was calculated with a three-dimensional beam attenuation code. Beam power had been previously calibrated with a calorimeter, and the beam species mix is taken from test stand measurements. The full-energy beam neutrals contribute 50% of the O VIII 102-Å intensity in the plasma center, while the one-half and one-third energy components each contribute 20%. The remaining 10% is accounted for by the beam-generated thermal (halo) neutrals.

The steady-state ( $t = 200 \text{ ms}$ ) radial profiles of  $C^{6+}$  and  $O^{8+}$  are shown in Fig. 3 along with model calculations which are discussed below. The error bars are the uncertainties in the average over the eight beam pulses. The more reliable

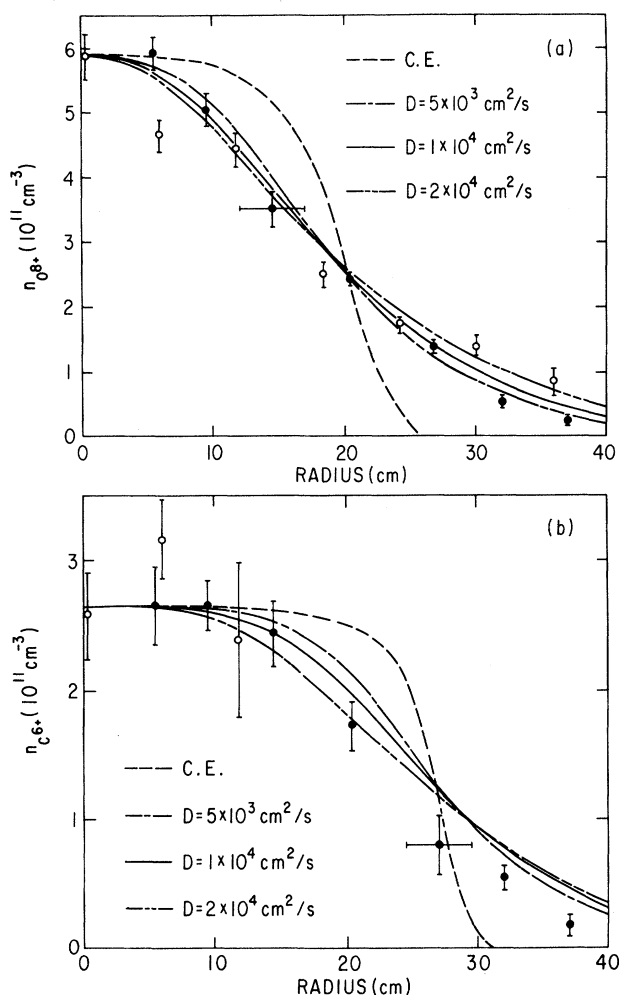


FIG. 3. Radial profiles of fully ionized oxygen and carbon during the steady-state phase of the discharge. Limiter radius is at 30 cm. Closed circles:  $R > R_{P1}$ . Open circles:  $R < R_{P1}$ .  $R_{P1} = 147$  cm. The solid lines are radial profiles of  $C^{6+}$  and  $O^{8+}$  calculated from an impurity transport code. C.E. denotes the distribution expected from coronal equilibrium assuming a constant impurity density.  $D$  is the constant impurity diffusion coefficient.

data are those at larger major radii (i.e., outside) where the beam has suffered less attenuation. The uncertainties in the absolute density scales in Fig. 3 are dominated by uncertainties in spectrometer calibration (30% to 50%), beam power, and charge-exchange cross sections. Ignoring contributions from all lower charge states (which can only serve to flatten the total density), the levels of  $n_{O^{8+}}$  and  $n_{C^{6+}}$  are, at most, slightly more peaked than  $n_e(r)$ , indicating no significant peaking of  $Z_{\text{eff}}$  on axis.

A noticeable feature of the  $O^{8+}$  and  $C^{6+}$  profiles

in Fig. 3 is that both fully stripped species have appreciable densities beyond the limiter radius at 30 cm. Since the electron temperature at the plasma edge is too low to produce  $C^{6+}$  and  $O^{8+}$ , impurity transport across the magnetic field in times short compared with the recombination times of 50 to 100 ms must be responsible for the presence of these ions at large radii.

The amount of cross-field transport necessary to account for the observed profiles can be estimated by comparison of the measured  $O^{8+}$  and  $C^{6+}$  radial distributions to those calculated with a multispecies impurity transport code.<sup>11</sup> The curves in Fig. 3 show results of steady-state calculations assuming either coronal equilibrium with a constant total impurity density or relatively simple diffusion models ( $\Gamma_q = -D \partial n_q / \partial r$ ). No parallel loss term was included in the scrapeoff region ( $r > 30$  cm).

Results from the TFR tokamak<sup>12</sup> seem to indicate that heavy impurities in the center of the discharge can be described by coronal equilibrium if the uncertainties in the various atomic rates are considered. In addition, the radial distribution of  $O^{8+}$  in the T-10 tokamak appears to be in agreement with coronal equilibrium,<sup>6</sup> albeit with quite large uncertainties in the data. In contrast, results from both the PDX<sup>13</sup> and PLT<sup>14</sup> tokamaks show deviations from coronal equilibrium for heavy impurities. Even with large uncertainties in the thermal neutral density, atomic rate coefficients, and plasma parameters, the  $O^{8+}$  and  $C^{6+}$  profiles reported here cannot be reconciled with coronal equilibrium. The measured profiles are in much better agreement with profiles calculated under the assumption of a constant diffusion coefficient of  $D = 10^4 \text{ cm}^2/\text{s}$ , which is the value obtained from analysis of earlier Sc injection experiments.<sup>13</sup>

Uncertainties in various plasma parameters, including  $n_e$ ,  $T_e$ , the thermal neutral density, scrapeoff parallel loss times, and other details, make it difficult to straightforwardly obtain rigorous transport results from the present data, and a wide range of  $D$  ( $\sim 5 \times 10^3$  to  $2 \times 10^4 \text{ cm}^2/\text{s}$ ) can give reasonable agreement with the observed profiles. It is clear that there is no strong central pinch effect on these ions. The purely diffusive model used here yields a constant total impurity density with radius in the core region ( $r < 30$  cm) where the source rate from recycling impurities is negligible. The uncertainties also allow the inclusion of a small inward velocity term in the flux sufficient to yield a roughly constant total

impurity concentration with radius. A more detailed transport analysis of these and other measurements will be reported later.

The intensity of the 102-Å line in the absence of the DNB is due to both electron excitation of  $O^{7+}$  and charge-exchange recombination of  $O^{8+}$  with the background thermal neutrals. The observed ratio of the modulated to steady-state signals at 102 Å is consistent with the transport-code results using a nominal thermal neutral density profile  $n_{Ho}(r)$  obtained from a neutral-particle transport code<sup>15</sup> [which gives  $n_{Ho}(0) \approx 2 \times 10^7 \text{ cm}^{-3}$ ]. However, a factor-of-3 uncertainty in  $n_{Ho}(r)$  precludes a reliable determination of the  $O^{7+}$  density from the measured 102-Å intensity. The influence of uncertainties in  $n_{Ho}(r)$  on the impurity ionization balance, and hence the calculated  $O^{8+}$  profiles, is less pronounced.

By assuming C and O to be the dominant impurity species and taking these ions to be fully stripped in the plasma center, the measured densities give  $Z_{\text{eff}} = 2.4 \pm 0.4$  at  $r = 0$ . The error estimate reflects the range of values obtained by using several (i.e., the 3-2 and 4-3) transitions in  $O^{7+}$  and  $C^{5+}$ . Plasma resistivity measurements give  $Z_{\text{eff}} = 2.1 \pm 0.2$  under the assumption of Spitzer resistivity, and visible bremsstrahlung measurements give  $Z_{\text{eff}} = 2.2 \pm 0.3$  at the plasma core. The value of  $Z_{\text{eff}}$  derived from the charge-exchange measurements is thus consistent with these other independently determined values. Unlike these other methods of determining  $Z_{\text{eff}}$ , the charge-exchange technique gives the added information of the ionic composition of the plasma. Estimates of the abundance of hydrogenic O in the plasma core would raise the quoted  $Z_{\text{eff}}$  by  $< 5\%$ . Metallic impurities (principally titanium) were negligible in these discharges.

The authors wish to acknowledge useful discus-

sions with E. Hinnov, D. Post, and S. Suckewer. Contributions from K. Bol, B. Grek, D. Johnson, S. Kaye, R. Reeves, and H. Towner are gratefully acknowledged. This work was supported by the U. S. Department of Energy under Contract No. DE-AC02-76-CHO-3073.

<sup>(a)</sup>Present address: Racah Institute of Physics, The Hebrew University, Jerusalem, Israel.

<sup>1</sup>R. C. Isler, Phys. Rev. Lett. **38**, 1359 (1977).

<sup>2</sup>R. C. Isler, L. E. Murray, S. Kasai, J. L. Dunlap, S. C. Bates, P. H. Edmonds, E. A. Lazarus, C. H. Ma, and M. Murakami, Phys. Rev. A **24**, 2701 (1981).

<sup>3</sup>S. Suckewer, E. Hinnov, M. Bitter, R. Hulse, and D. Post, Phys. Rev. A **22**, 725 (1980).

<sup>4</sup>W. H. M. Clark *et al.*, Nucl. Fusion **22**, 333 (1982).

<sup>5</sup>V. V. Afrosimov, Yu. S. Gordeev, A. N. Zimov'ev, and A. A. Korotov, Fiz. Plazmy **5**, 981 (1979) [Sov. J. Plasma Phys. **5**, 551 (1979)].

<sup>6</sup>A. N. Zimov'ev, A. A. Korotko, E. R. Krzhizhanovskii, V. V. Afrosimov, and Yu. S. Gordeev, Pis'ma Zh. Eksp. Teor. Fiz. **32**, 557 (1980) [JETP Lett. **32**, 539 (1980)].

<sup>7</sup>A. Nudelman, R. Goldston, and R. Kaita, to be published.

<sup>8</sup>T. A. Green, E. J. Shipsey, and J. C. Browne, Phys. Rev. A **23**, 546 (1981).

<sup>9</sup>A. Salop, J. Phys. B **12**, 919 (1979).

<sup>10</sup>H. Ryufuku and T. Watanabe, Phys. Rev. A **18**, 2005 (1978).

<sup>11</sup>R. A. Hulse, to be published.

<sup>12</sup>TFR Group, Association EURATOM-Commissariat à l'Energie Atomique Report No. EUR-CEA-FC-1033, 1980 (unpublished).

<sup>13</sup>R. Hulse, K. Brau, J. Cecchi, S. Cohen, M. Finkenthal, R. Fonck, D. Manos, and S. Suckewer, Bull. Am. Phys. Soc. **26**, 864 (1981).

<sup>14</sup>E. Hinnov, in *Atomic and Molecular Processes in Controlled Thermonuclear Fusion*, edited by M. R. C. McDowell and A. M. Ferendeci (Plenum, New York, 1980), pp. 449-470.

<sup>15</sup>S. Tamor, J. Comput. Phys. **40**, 104 (1981).